https://doi.org/10.1016/j.enconman.2020.112868

Techno-economic design optimization of hybrid renewable energy applications for high-rise residential buildings

Jia Liu [a], Meng Wang [b], Jinqing Peng [c], Xi Chen [a, d*], Sunliang Cao [a], Hongxing Yang [a*]

[a] Renewable Energy Research Group (RERG), Department of Building Services Engineering,
The Hong Kong Polytechnic University, Kowloon, Hong Kong, China

[b] School of Energy and Power Engineering, Changsha University of Science and Technology, Changsha, Hunan, China

[c] College of Civil Engineering, Hunan University, Changsha, Hunan, China

[d] School of Science and Technology, The Open University of Hong Kong, Hong Kong, China

Abstract

This study aims to explore the techno-economic feasibility of renewable energy systems for power supply to high-rise residential buildings within urban contexts. Experiments on a photovoltaic (PV) and battery storage system under maximizing self-consumption and time-of-use strategies are conducted to study the system performance and validate energy balance based battery and energy management models. Four renewable application scenarios are investigated for a typical high-rise building in Hong Kong through coupled modelling and optimizations with TRNSYS and jEPlus+EA. A comprehensive technical optimization criterion integrating the energy supply, battery storage, building demand and grid relief indicators is developed, and the levelized cost of energy (LCOE) considering detailed renewables benefits including the feed-in tariff, transmission loss saving, network expansion saving and carbon reduction benefit is formulated. Experimental results show that root mean square deviations between the tested and simulated battery state of charge for the two strategies are 1.49% and 0.94% respectively. It is indicated that the PV system covers 16.02% of the annual load at a LCOE of 0.5252 US$/kWh and the PV-wind system covers 53.65% of the annual load at the lowest LCOE of 0.1251 $/kWh. The added battery improves the annual average load cover ratio and self-consumption ratio by 14.08% and 16.56% respectively, while the optimum PV-wind-battery system covers 81.29% of the annual load at an affordable LCOE of 0.2230 $/kWh. Techno-economic analyses of different typical scenarios can provide valuable references to related stakeholders for a promotion of renewable applications in high-rise buildings and further reduction of urban carbon footprint.

* Corresponding author1: climber027@gmail.com; patrick.x.chen@connect.polyu.hk
* Corresponding author2: hong-xing.yang@polyu.edu.hk

Keywords: Solar photovoltaic; Wind turbine; Battery storage; Multi-objective optimization; Urban context

1. Introduction

1.1. Background

The Paris Agreement calls for global efforts to achieve carbon neutrality before 2100 and control the global average temperature rise below 2°C based on the pre-industrial level [1]. Ambitious plans are made in different countries and regions to take positive measures to support this agreement. For example, a comprehensive climate action plan is implemented in Hong Kong to reduce the carbon footprint to 3.3 - 3.8 tonnes/capita by 2030 with a 65% - 70% decline compared with 2005's level [2]. It is reported that the major part of emissions in a country can be attributed to just one or several domestic cities, where Hong Kong ranks the second largest carbon consumer in China [3]. Therefore, it is of great importance to adopt decarbonisation measures in Hong Kong to significantly reduce carbon emissions.

Renewable energy applications in cities have promising potential to reduce carbon emissions [4] and air pollution [5], while maintaining a sustainable energy supply [6]. They are attracting increasing attention in urban developments with a continuously decreasing cost and ever growing social and environmental benefits in recent years [7, 8]. Among these applications, solar photovoltaic (PV) shows a rapid cost decline in the module price by more than 90% since 2010. Especially, the crystalline silicon module price was lowered by 26% - 32% from 2017 to 2018. The wind power also experienced a cost decline with the turbine price dropped by 10% - 20% since 2017. The global weighted average levelized cost of energy (LCOE) of the solar PV, onshore wind and offshore wind all declined in 2018 by 13%, 13% and 1% respectively since 2017 due to the technology improvement, installation cost decline and increasing market competition [9]. It is reported that over 100 cities worldwide are 70% powered by renewable electricity by the end of 2018 and at least 40 cities are powered by 100% renewables. Moreover, an increasing number of cities are setting ambitious targets for 100% renewable electricity in one or more sectors [10].

To develop renewable energy for power supply to buildings in a high-density city such as Hong Kong is important as its building sector accounts for over 90% of the total electricity consumption which is equivalent to over 60% of local carbon emissions. About 3% - 4% of the renewable energy potential from wind, solar and waste-to-energy sources is anticipated in Hong Kong by 2030, with 1% equals to up to 440 million kWh electricity supporting 90,000 households [2]. To fully utilize unstable renewable power such as intermittent solar and wind dependent on weather conditions, the battery storage technology is introduced to couple with renewable sources to match with the building load [11]. The battery storage applied in renewable systems can not only improve energy autonomy and flexibility of renewable systems [12], but also benefit the grid relief with less power exchange with the utility grid [13]. The accumulated global battery storage capacity excluding small-scale installations reached over 3 GW in early 2019, leading to a further price drop of the utility-scale by 40% through 2018 on top of the 80% reduction between 2010 and 2017 [9]. Therefore, it is promising to apply renewable energy and battery storage systems to power supply for buildings within urban context such as Hong Kong [14] with the continuous technology improvement and cost reduction.

1.2. Literature review

Recently, a large number of studies have been conducted on the design optimization of renewable energy and electric energy storage (RE-EES) systems for power supply to buildings and communities in both urban and remote regions.

Much attention has been paid to sizing and optimizing RE-EES systems for power supply to single buildings in urban areas. The grid-connected PV-wind system with and without battery storage is studied for electric power supply to a residential building in an Italian city with TRNSYS 17. The Pareto-front and energy reliability-constrained methods are used to achieve the optimum energy reliability of the renewable energy system [15]. The lifecycle cost and carbon emissions of a one-floor building in The Bahamas are investigated by optimizing the building envelope and energy supply from the PV-battery system. In this study, the Percentage of Persons Dissatisfied of building occupants is treated as constraints in the optimization process with the co-simulation and optimization platform of EnergyPlus and jEPlus+EA. It clarifies the feasibility to develop renewable energy systems for residential buildings in The Bahamas [16]. The PV system is also developed as one of the energy retrofit measures to achieve the optimal performance on the energy demand, cost and carbon emissions for a low-density residential building located in 19 selected European cities. The Active Archive Non-dominated Sorting Genetic Algorithm (aNSGA-II type) is adopted to realize the optimization process in the joint simulation and optimization environment of EnergyPlus and Python. This study concludes that the application of solar energy is the most convenient solution for building retrofitting [17].

In addition to applying RE-EES systems to single buildings, urban community applications are also studied by researchers. The building envelope and renewable supply systems of a residential complex with five buildings in Italy are optimized to minimize the global cost and air-conditioning load [18]. Waibel et al. investigated the influence of building geometry on the cost and carbon emissions for four office blocks with PV-battery systems in Switzerland [19]. A hybrid PV-wind-battery system is developed for a municipality building with six blocks in Portugal by optimizing the total cost of energy considering various feed-in tariff (FiT) schemes. It is indicated that the developed mixed integer linear programing is feasible for evaluating renewable energy systems in zero energy buildings [20]. A systematic and integrative decision-making method is also presented to find the cost-optimal solution for a microgrid PV-wind-battery-fuel cell (FC)-diesel system installed in an urban community of Egypt [21].

Furthermore, optimization work is also conducted on RE-EES systems for buildings and communities in remote area without grid access. An off-grid PV-wind-battery system is optimized to achieve the minimum total present cost and loss of power supply probability (LPSP) for a house in Tehran. The study adopts genetic algorithm with particle swarm optimization (GA-PSO) and multi-objective particle swarm optimization (MOPSO) methods to achieve an optimum LCOE of 0.508 $/kWh [22]. An improved crow search algorithm (CSA) is proposed to size an off-grid PV-diesel-FC system to achieve the minimum total net present cost with the LPSP and renewable energy portion as constraints. It indicates that the hybrid system is reliable and economic to meet the electrical load of a remote building in Kerman [23]. The PV-wind-battery for a remote island with ten houses is sized with a novel mathematical model introducing a saturation factor of each renewable energy resource. This study shows that a 2 kW wind turbine is the most cost-effective installation for the island and the wind-alone system performs better than the solar-alone system [24]. An off-grid PV system coupled with the hydrogen storage and retired electric vehicle (EV) is developed for power supply to a small neighborhood of ten houses in China on the HOMER platform. It is found that the Non-dominated sorting Genetic Algorithm-II (NSGA-II) method is superior to the multi-objective evolutionary algorithm based on decomposition (MOEA/D) for minimizing the loss of power supply, economic cost and potential energy waste [25].

Table 1 Recent optimization sizing studies on renewable energy systems for buildings

Renewable system	Application site	Optimization method	Simulation platform	Optimization objective	Reference
On-grid PV-wind-battery	An urban residential building, Italy	Pareto-front method, energy reliability-constrained method	TRNSYS	Energy reliability	Mazzeo et al. 2018 [15]
On-grid PV-battery	A one-floor home, The Bahamas	NSGA-II	EnergyPlus, jEPlus+EA	Lifecycle cost, carbon emission	Bingham et al. 2019 [16]
On-grid PV	A residential building, 19 Europe cities	aNSGA-II type	EnergyPlus, Python	Demand, costs, carbon emission	Salata et al. 2020 [17]
On-grid PV	Residential complex (five buildings), Italy	PSO	TRNSYS, GenOpt	Global cost, heating/cooling demand	Ferrara et al. 2019 [18]
On-grid PV-battery	Four office buildings, Switzerland	Radial Basis Function Optimization	EnergyPlus, Rhinoceros 3D, Grasshopper	Operational cost, carbon emission	Waibel et al. 2019 [19]
On-grid PV-wind-battery	Six building blocks, Portugal	Mixed integer linear programing model	General Algebraic Modeling System	Total economic cost	Rosa et al. 2018 [20]
Microgrid PV-wind-battery-FC-diesel	Urban community, Egypt	Systematic and integrative decision-making method	HOMER Pro	Total net present cost	Elkadeem et al. 2020 [21]

Renewable system	Application site	Optimization method	Simulation platform	Optimization objective	Reference
Off-grid PV-wind-battery	A house in Tehran, Iran	GAPSO	HOMER	Total present cost, LPSP	Ghorbani et al. 2018 [22]
Off-grid PV-diesel-FC	A remote building in Kerman, Iran	Crow search algorithm	MATLAB	Total net present cost	Ghaffari, Askarzadeh. 2020 [23]
Off-grid PV-wind-battery	Ten-house remote island, China	Mathematical model	MATLAB	Net present cost, simple payback time, LPSP	Ma et al. [24]
Off-grid PV-FC-EV	Ten-house neighborhood, China	NSGA-II, MOEA/D	HOMER	Loss of power supply, cost, energy waste	Huang et al. 2019 [25]

The recent optimization sizing studies on RE-EES systems for building applications are compared in Table 1 based on the detailed optimization methods and objectives for different building/community applications. It indicates that the system cost is a primary objective adopted by many researchers and the energy reliability of renewable supply systems is also widely concerned. The environmental impact, as evaluated by carbon emissions, has attracted increasing attention given the contribution of renewable energy systems to the sustainable development as a promising alternative fuel. Based on the brief literature review, research gaps can be identified in evaluating the comprehensive performance of the energy supply, storage, demand and grid integration when optimizing and sizing RE-EES systems for building applications. Moreover, few studies have considered the potential benefits from the transmission loss saving, network expansion saving, and carbon reduction when evaluating the cost of energy for renewable applications in high-rise buildings within urban contexts. In addition, many simulation studies are not validated by field experiments in terms of storage models and energy management strategies.

1.3. Scope and contribution

This study firstly conducts field tests on an experimental PV-battery system to explore its operational performance and validate the energy balance based battery and energy management strategy models in TRNSYS. Secondly, four typical renewable energy application scenarios for power supply to a typical high-rise residential building in Hong Kong are developed and sized with the coupled modelling and optimization platform of TRNSYS and jEPlus+EA. The contribution of the present study includes:

(1) Experiments on the PV-battery system are conducted to validate the energy balance based battery model and energy management strategy for TRNSYS modelling.

(2) An integrated technical optimization criterion is developed considering the energy supply, battery storage, building demand and grid relief performance of PV-wind-battery systems for the technical feasibility assessment of a high-rise residential building.

(3) Detailed benefits of renewable energy systems for urban building applications are considered in the LCOE evaluation covering the FiT subsidy, transmission loss saving, network expansion saving and carbon reduction benefit.

(4) The technical and economic feasibility of four typical renewable energy application scenarios is compared and discussed for high-rise buildings in Hong Kong to provide guidance for stakeholders to promote the penetration of renewable energy into urban areas.

2. Methodology

The framework of this research involving both experiments and simulations is illustrated in Fig. 1. Experiments on a test building platform with the PV-battery system are conducted to study the system operational performance and validate the energy balance based battery and energy management strategy (EMS) for TRNSYS modelling. The building-integrated PV (BIPV) system with both rooftop and façade installations is firstly developed for the typical high-rise building as Case 1. BIPV is combined with wind power in Case 2 to achieve the annual energy balance of the supply and demand as PV power alone cannot cover the total building demand. The battery is introduced and optimized in Case 3 to improve the match of PV-wind power with the residential electrical load. The wind power and battery capacity are jointly sized and optimized in Case 4 to find a techno-economic optimum solution for the high-rise building. An integrated technical optimization criterion focusing on the energy supply, building demand, battery storage and grid relief performance is developed for technical feasibility assessment.

And a comprehensive LCOE covering detailed benefits of the renewable system including the FiT subsidy, transmission loss saving, network expansion saving and carbon reduction benefit is formulated for economic feasibility assessment. The final optimum solution is solved by the minimum distance to the utopia point method on top of the obtained Pareto Frontier from a multi-criterion design optimization [19].

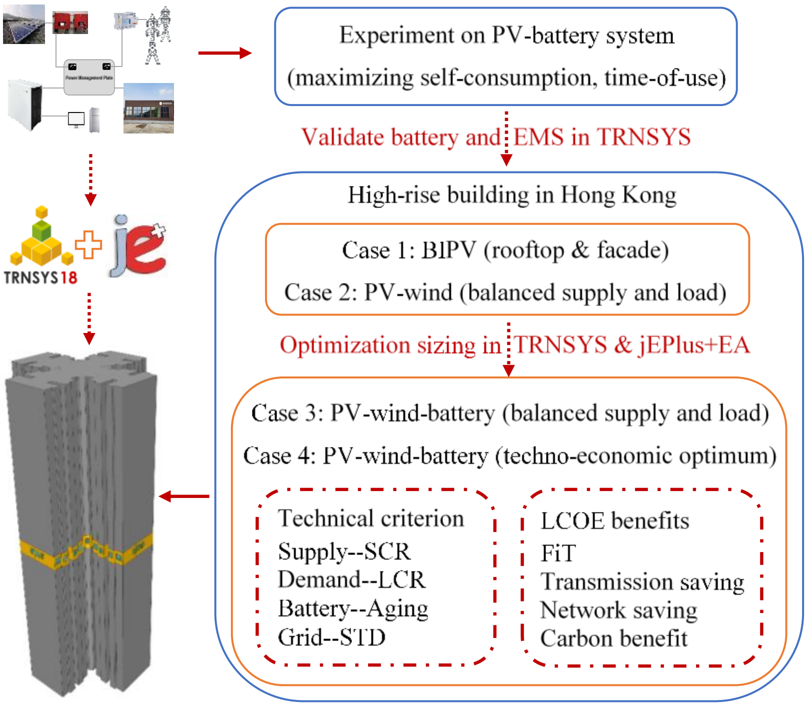

Fig. 1 Framework of renewable energy applications for high-rise buildings

2.1. Experimental tests of the PV-battery system

Experiments on the PV-battery system are carried out on a test platform in Hunan to study the system operational performance under two widely-used energy management strategies (maximizing self-consumption and time-of-use strategies). TRNSYS models of the tested PV-battery system under the two strategies are established based on the collected power data. And the dynamic test and simulation results of battery (state of charge) SOC are then analyzed and compared to validate the battery model and energy management strategies based on the energy balance mechanism for TRNSYS modelling. The energy balance based battery model and energy management strategy are independent of locations and weather conditions. And then the validated battery model and the most widely-used strategy (maximizing self-consumption) are used to study the technical and economic feasibility of renewable energy systems for a typical high-rise building in Hong Kong.

Fig. 2 Testing platform with PV-battery system

Polysilicon PV panels are installed on the rooftop of the test building with a rated capacity of 305 W × 30 modules as shown in Fig. 2. And a 12 kWh lithium-ion battery with the life span of 6,000 cycles is matched to store surplus renewable power in off-peak periods and discharge to meet the building load in peak hours when renewable power is not enough. Specific parameters of the PV-battery system are shown in Table 2.

Table 2 Specification of the PV-battery system

Solar module	SK6612P-305 (Polysilicon)
Rated maximum power	305 W
Voltage at P_{max}	36.5 V
Current at P_{max}	8.35 A
Open-circuit voltage	45.3 V
Short-circuit current	8.94 A
Normal operating cell temperature	47±2°C
Maximum system voltage	1,000 V
Dimension	1,957*992 mm
Rooftop module number	30
Battery	MINIES-P90B12-E-R2 ($LiFePO_4$)
Rated capacity	12 kWh
Maximum on-grid power	9 KVA
Operational SOC	15% - 98%

Size	738(W)*598(D)*1,070.5(H) mm
Inverter	GW5000-DT
Nominal output power	5,000 W
Maximum direct current input power	6,500 W
Maximum power point tracking range	200 - 800 V

A schematic diagram of the grid-connected PV-battery system is shown in Fig. 3. Two inverters (GW5000-DT) are connected to rooftop PV panels with a conversion efficiency of 95%. A grid meter is installed to measure the power flow from the utility grid (positive: power supply from the grid, negative: power fed into the grid). The inverter signal and grid signal are collected by Hall sensors and connected into the power distribution plate, which are also linked to the battery bank. The target active power of the battery is controlled according to the difference of the dynamic PV power and electrical load.

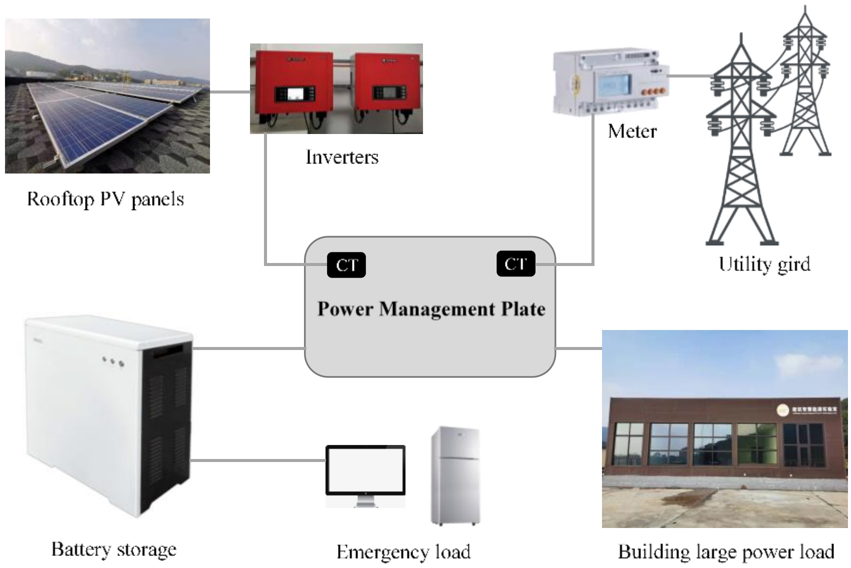

Fig. 3 Schematic of the grid-connected PV-battery system

Two basic energy management strategies including the maximizing self-consumption strategy (Fig. 4(a)) and time-of-use strategy (Fig. 4(b)), are developed and input into the power management plate to control the power operation of the PV-battery system.

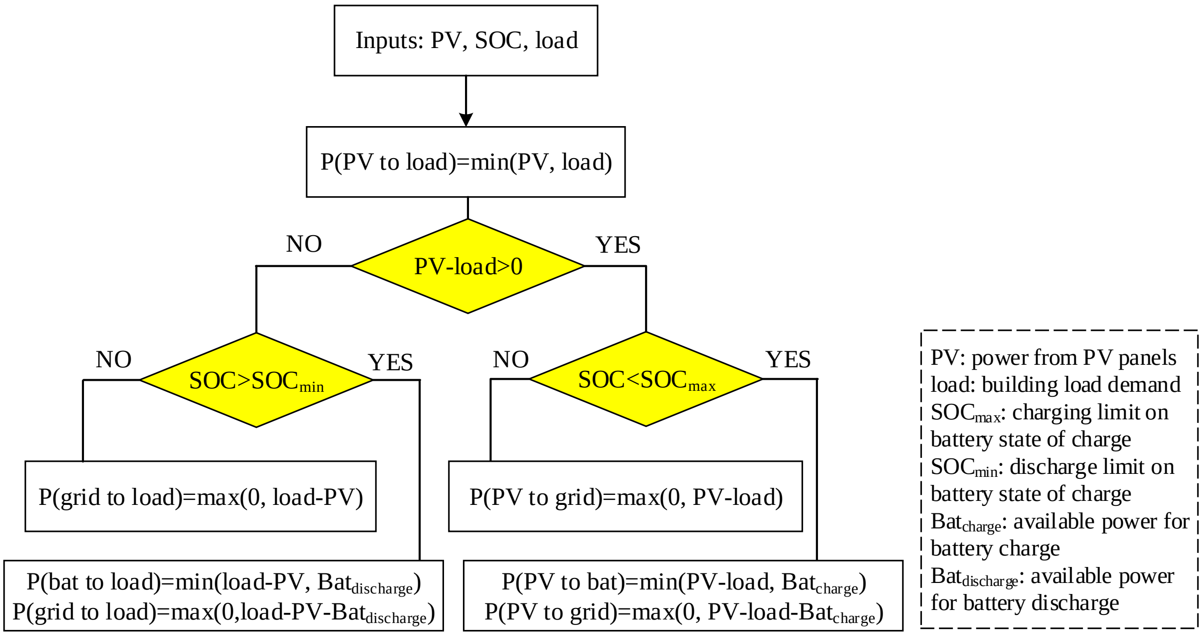

Fig. 4(a) Energy management strategy - maximizing self-consumption strategy

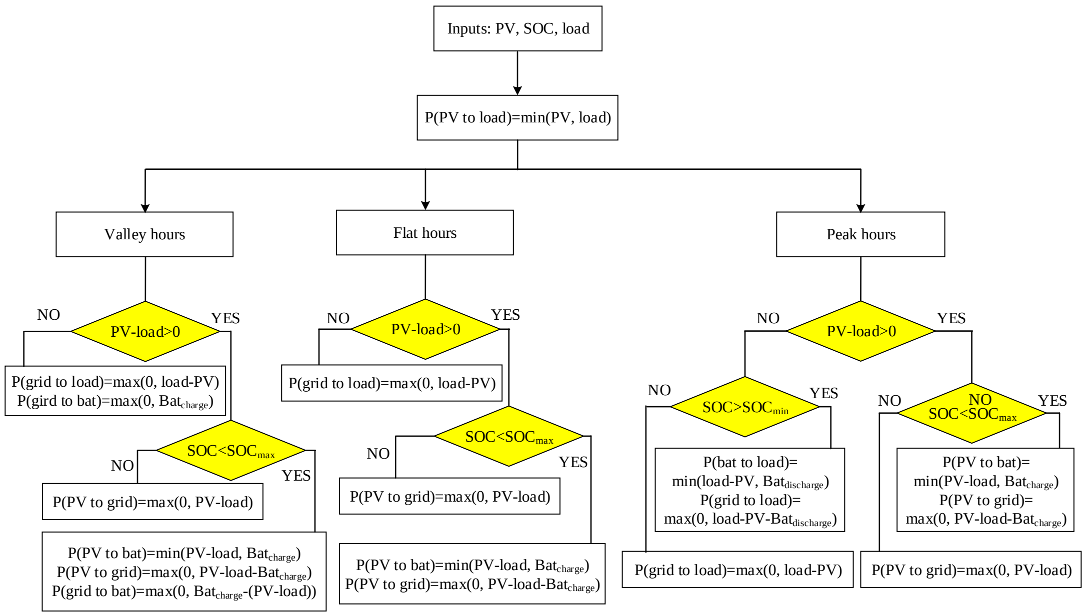

Fig. 4(b) Energy management strategy - time-of-use strategy

The first tested basic energy management strategy aims to maximize the self-consumption ratio of the PV-battery system. Three days (15 - 17 December 2019) with different weather conditions in Hunan are chosen to test the maximizing self-consumption strategy. The second realized strategy is the time-of-use strategy operated during 18 - 20 December 2019 and the dynamic PV power output during these six testing days is shown in Fig. 5.

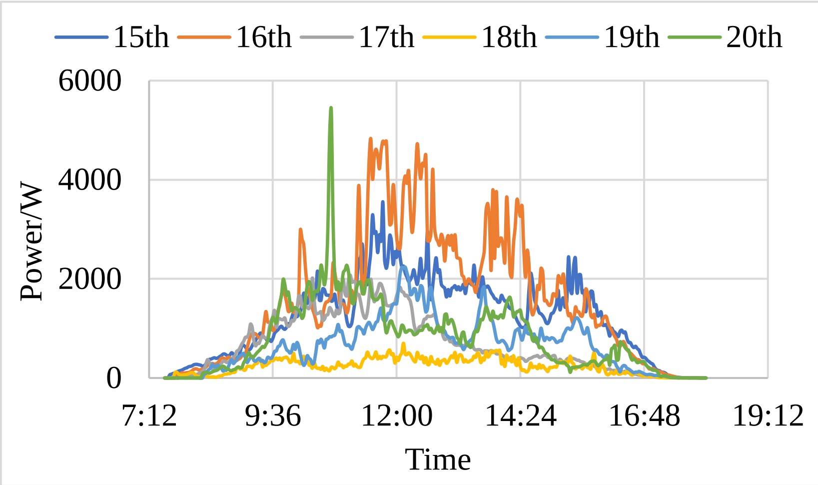

Fig. 5 PV power output during six experimental days

The dynamic PV generation, load power, grid power and battery SOC are collected to show the system performance for different strategies and to validate the battery and energy management models for TRNSYS modelling based on the energy balance mechanism. The validated battery model and maximizing self-consumption strategy are then adopted to study renewable energy applications for a typical high-rise building in Hong Kong.

2.2. Modelling of renewable energy systems for a typical high-rise residential building

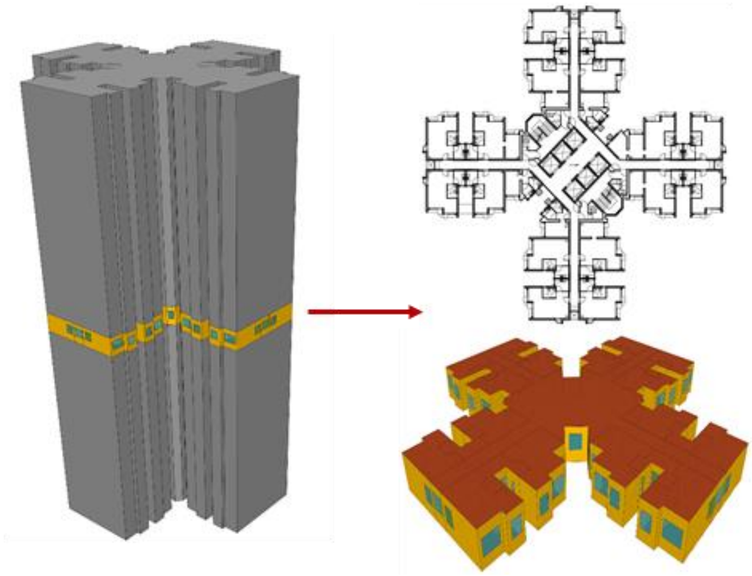

Fig. 6 Floor layout of the residential building

A high-rise residential building of 30 floors is constructed with a typical floor layout of the New Harmony One design from the public rental housing in Hong Kong. It is reported that about 30% of the population in Hong Kong live in the public rental housing which widely adopts this standard design plan in new developments [26]. There are eight one-bedroom units designed for two occupants and eight two-bedroom units designed for four occupants in each floor as shown in Fig. 6. The building is firstly established in SketchUp and then imported to TRNSYS 18 to generate the load profile. The detailed parameters of the building envelope are shown in Table 3 according to the local design code [27, 28].

Table 3 Thermal properties of the residential building

Building envelope	Material	Thickness (m)	Thermal conductivity (W/mK)
External wall	Gypsum plastering	0.01	0.38
	Heavy concrete	0.1	2.16
	Cement/sand plastering	0.01	0.72
	Mosaic tiles	0.005	1.5
Internal wall	Gypsum plastering	0.02	0.38
	Heavy concrete	0.13	2.16
	Gypsum plastering	0.02	0.38
Floor	Heavy concrete	0.1	2.16
	Cement screed	0.025	0.72
	Plastic tiles	0.005	1.5
Roof	Gypsum plaster	0.01	0.38
	Heavy concrete	0.15	2.16
	Expanded polystyrene	0.05	0.034
	Cement/sand screed	0.05	0.72
	Asphalt	0.02	1.15
	Concrete tiles	0.025	1.1
Window	Tinted glass	0.006	1.05

The ventilation, air conditioning, occupancy, equipment and lighting profiles are set based on the local design code published by Hong Kong Electrical and Mechanical Services Department [29]. The detailed load is modeled by internal components of the TRNSYS library including Type 56, Type 648, Type 667, Type 752, Type 655 and other auxiliary units. Type 15 is used to provide weather data of a typical meteorological year for the building load estimation.

The simulation of the high-rise residential building is conducted at a time step of 0.125 h and the load results of the whole year and July are shown in Table 4. It is found that the average air-conditioning load of the building is 43.99 kWh/m^2 and the average hot water load is about 46.51 kWh/m^2 comparable to that of air conditioning. The modelled building results agree with the survey results reported by Wan et.al that the reliable ranges of the average annual air-conditioning and hot water electricity consumption in standard public rental housing blocks in Hong Kong are 40 - 45 kWh/m^2 and 41 - 50 kWh/m^2 [30]. The total building load in the typical year and seventh month is 129.33 kWh/m^2 and 13.66 kWh/m^2 respectively.

Table 4 Load demand modelling results of the high-rise residential building

Building load	Annual	July
Internal gain load, kWh	559,506.67	47,534.66
Internal gain load per unit area, kWh/m^2	38.84	3.30
Air conditioning load, kWh	633,699.28	104,041.23
Air conditioning load per unit area, kWh/m^2	43.99	7.22
Hot water load, kWh	670,055.50	45,290.16
Hot water load per unit area, kWh/m^2	46.51	3.14
Building total load, kWh	1,863,261.46	196,866.05
Building total load per unit area, kWh/m^2	129.33	13.66

Renewable energy systems are considered for power supply to this typical high-rise residential building in Hong Kong based on four typical application scenarios as below:

Case 1: PV panels are applied to both the rooftop and façades and is not able to cover all the electrical load of the high-rise building.

Case 2: Both PV and wind power are introduced to achieve an annual energy balance between the building electrical load and renewable energy supply.

Case 3: The battery storage technology is applied to the PV-wind supply system with balanced annual supply and demand to improve the load matching, and the multi-objective optimization is conducted to determine an appropriate battery capacity considering the techno-economic performance of the system.

Case 4: The wind capacity and battery capacity are simultaneously optimized in the hybrid

PV-wind-battery system to find a comprehensive techno-economic optimum solution based on the multi-objective optimization and decision-making approach.

The rooftop PV panels are modelled by TRNSYS Type 103 with the maximum power point tracked at a tilted angle of 22º close to the latitude of Hong Kong [31]. And the PV panels are also installed on the four facades of the building to achieve a maximum building-integrated renewable energy generation. Type 567 in the TRNSYS library is adopted to simulate the façade PV modules according to the empirical equivalent circuit model and algorithm developed by Duffie and Beckman [32] considering different azimuths of installed facades. An adjacent shading factor of 76.64% is considered for façade PV panels compared with a standalone baseline building to address the high-density urban environment in Hong Kong [33]. The wind turbine is simulated by TRNSYS Type 90 and external operation parameters from wind turbine manufactures are adopted to provide power and wind speed characteristics [34]. The transmission loss of the wind power [35] is considered as it is used for buildings in urban areas far away from the wind power plant. The battery energy storage is modelled according to the energy balance mechanism considering the battery cycling aging and the battery SOC formulated as Eq. (1) is controlled to maintain within operational limits.

$$SOC_i = SOC_0 + \frac{\int P_{battery}}{Battery_{rated} \cdot SOH} \tag{1}$$

where $P_{battery}$ is the power flow of the battery in the charge and discharge process with opposite values, kW. $Battery_{rated}$ is the battery rated capacity, kWh. SOH is the battery state of health (SOH) degrading from the full usable capacity of 100% SOH to 80% SOH as the end of its life considering the cycling aging as shown in Eq. (2) [36].

$$cycling\ aging_i = aging_0 + 0.5 \cdot \frac{\int |P_{battery}|}{Battery_{rated}} \cdot \frac{1}{Equ_{lifecycle}} \tag{2}$$

where $Equ_{lifecycle}$ is the battery equivalent lifecycle number, 6,000 cycles for the lithium-ion battery adopted in this study [37].

The renewable energy systems are connected to the utility grid to import electricity to meet the unsatisfied load or export surplus renewable power into the grid. The maximizing self-consumption strategy as validated by the experiment is adopted as the energy management method of all studied cases. When surplus renewable energy is available after meeting the building demand, it will be controlled to charge the battery until reaching the maximum SOC and then fed into the grid. When the electrical load in the building cannot be satisfied by renewable sources, the battery will be discharged to cover the load until reaching the minimum SOC and then the grid supply will meet the load. Design parameters of the renewable systems are shown in Table 5.

Table 5 Parameters of renewable energy systems for the high-rise building

System component	Rooftop PV	Facade PV	Wind turbine	Battery storage	Inverter/ converter
Installed capacity	70.76 kW	805.95 kW	Case determined	Case determined	--
Annual output per unit power kWh/W	1.215	0.461	--	--	--
Annual output per unit area kWh/m^2	218.019	69.114	--	--	--
Initial cost (cover installation)	3,500 $/kW	3,500 $/kW	4,000 $/kW	1,000 $/kWh	700 $/kW
Maintenance (ratio of initial cost) [38]	2%	2%	1%	1%	1%
Lifetime, year	20	20	20	5	10

It shows that 70.76 kW PV panels can be installed on the rooftop of the high-rise building excluding the required area for roof maintenance. And the annual output of the rooftop PV installation is 1.215 kWh/W and 218.019 kWh/m^2. PV panels are also installed on four façades of the high-rise building considering an adjacent shading factor of 76.64% with a standalone building as the baseline [33], leading to much lower annual power generation about 0.461 kWh/W.

2.3. Multi-objective optimization for sizing hybrid PV-wind-battery systems

To size the battery capacity in Case 3 and optimize the wind and battery capacity in Case 4, the multi-objective optimization method is adopted to find techno-economic optimum solutions based on the coupled simulation and optimization platform of TRNSYS and jEPlus+EA. An integrated technical optimization criterion covering the performance of the energy supply, battery storage, building demand and grid relief is developed. And the LCOE is evaluated as the economic criterion considering detailed benefits of applying renewables in urban areas including the FiT subsidy, transmission loss saving, network expansion saving and carbon reduction benefit.

2.3.1. Optimization methods and design variables

The Non-dominated Sorting Genetic Algorithm-II (NSGA-II) is adopted to solve the multi-objective optimization problem given its robustness and efficiency as well as the smooth integration with TRNSYS [16]. The NSGA-II program improves the adaptive fit of candidate populations based on the sorting method of Pareto dominance with a set of constrains and objectives. The population size is set as 10 and the maximum generation is set as 200 to ensure a comprehensive searching range [39]. The crossover probability and mutation probability is 0.9 and 0.05 respectively to keep a balance between the convergence speed and spreading of the solution space [40].

The battery capacity is the only optimization variable in Case 3 as the building-integrated rooftop and façade PV capacity are fixed by the building geometry while wind power is determined by the annual energy balance between the renewable power generation and building electrical load. Both the battery capacity and wind power capacity are selected as optimization variables in Case 4 to find a comprehensive optimum solution for the hybrid PV-wind-battery system applied in the high-rise building. The variation range of the battery capacity installed in the building is 120 - 2,400 kWh (4 - 80 kWh/floor). And the increment of the battery capacity is 120 kWh (4 kWh for each floor with four units). The number of wind turbines at a rated capacity of 100 kW each is selected as the other optimization variable with a changing range of 1 - 20 at an increment of 1.

2.3.2. Techno-economic optimization criteria

In terms of the technical performance assessment of the hybrid PV-wind-battery system, an integrated criterion covering the energy supply, battery storage, building demand and grid relief indicator is proposed. And the improved LCOE is formulated to assess the economic feasibility considering detailed benefits of renewable energy applications including the FiT subsidy, transmission loss saving, network expansion saving and carbon reduction benefit.

(1) Integrated technical optimization criterion

Four important indicators regarding the four major components of the system are considered as an integrated technical criterion, namely the renewable energy self-consumption ratio (SCR) to evaluate the energy supply performance, the battery cycling aging (Aging) for storage evaluation, the load cover ratio (LCR) for demand assessment, and the standard deviation (STD) of net grid power for grid relief evaluation.

To evaluate the energy supply performance of the hybrid system, the annual average renewable energy SCR is calculated by Eq. (3).

$$RE\ self\text{-}consumption\ ratio = \frac{self\text{-}consumed\ RE\ electricity}{total\ electricity\ generation\ from\ RE} = \frac{E_{RE\ to\ load} + E_{RE\ to\ battery}}{E_{RE}} \quad (3)$$

where E_{RE_load} is the total annual electricity from PV panels and wind turbines to meet the building load, kWh. $E_{RE\_battery}$ is the total annual renewable electricity to charge the battery, kWh. E_{RE} is the annual power generation of PV panels and wind turbines, kWh.

The battery cycling aging dependent on the rated energy capacity and life cycle number is considered to assess the battery state of health degrading from the full usable capacity of 100% state of health to 80% state of health as the end of its life as shown in Eq. (4) [36] as explained in Section 2.2.

$$cycling\ aging_i = aging_0 + 0.5 \cdot \frac{\int |P_{battery}|}{Battery_{rated}} \cdot \frac{1}{Equ_{lifecycle}} \quad (4)$$

The annual average LCR is defined as the ratio of the provided electricity of renewable systems to the total annual building electrical load as shown in Eq. (5).

$$load\ cover\ ratio = \frac{Renewable\ system\ provided\ electricity}{total\ electricity\ demand} = \frac{E_{RE\ to\ load} + E_{battery\ to\ load}}{E_{load}} \quad (5)$$

where $E_{battery\ to\ load}$ is the battery electricity discharged to the building load, kWh. E_{load} is the total annual electrical demand of the building, kWh.

In terms of the grid relief, STD of net grid power is evaluated as per in Eq. (6) [41].

$$Average\ grid\ stress_{year} = STD(P_{grid\ to\ load} - P_{RE\ to\ grid})_{step} \quad (6)$$

where $P_{grid\ to\ load}$ is the grid exported power to meet the electrical load, kW. $P_{RE\ to\ grid}$ means the renewable power fed into the utility grid, kW.

These four technical indicators are normalized and integrated as an overall technical optimization criterion using the weighted sum method [42, 43] by assigning the same weighting as these four technical indicators are considered to be equally important to sizing the hybrid PV-wind-battery system as shown in Eq. (7).

$$Technical_{optimal} = LCR_{normalized} + SCR_{normalized} + Aging_{normalized} + STD_{normalized} \quad (7)$$

(2) Economic optimization criterion with detailed renewables benefits

To evaluate the economic feasibility of renewable energy systems for power supply to high-rise buildings, an improved LCOE considering the investment costs (including the initial cost, replacement cost, maintenance cost and residual cost) and detailed benefits (covering the FiT subsidy [44], transmission loss saving, network expansion saving and carbon reduction benefit) according to local regulations is formulated by Eq. (8).

$$LCOE = \frac{(PRV_{costs} - PRV_{benefits})}{\sum_{n=1}^{n=N} \frac{E_{PV} \cdot (1-\delta_{PV})^{n-1}}{(1+i)^n} + \sum_{n=1}^{n=N} \frac{E_{WT} \cdot (1-\delta_{WT})^{n-1}}{(1+i)^n}} \quad (8)$$

where PRV_{costs} is the present value of the investment costs including the initial cost (PRV_{ini}), replacement cost (PRV_{rep}), maintenance cost ($PRV_{O\&M}$) and residual cost (PRV_{res}) of major system components (i.e. PV panels, wind turbines, batteries and inverters) as shown in Eq. (9). $PRV_{benefits}$ is the present value of potential benefits of renewable energy systems including the FiT subsidy, transmission loss saving, network expansion saving and carbon reduction benefit as shown in Eq. (10). n is a certain year in the lifetime and N is the total system service lifetime, 20 years in this study. E_{PV} is the PV energy generation in the first year, kWh. δ_{PV} is the annual degradation rate of the PV system. E_{WT} is the wind energy generation in the first year, kWh. δ_{WT} is the degradation rate of the wind turbine system. i is the annual real discount rate.

$$PRV_{costs} = PRV_{ini} + PRV_{rep} + PRV_{O\&M} - PRV_{res}$$

$$= C_{ini} + \sum_{j=1}^{j=J} C_{ini} \left(\frac{1-d}{1+i}\right)^{j \cdot l} + \sum_{n=1}^{n=N} \frac{f_{mai} \cdot C_{ini}}{(1+i)^n} - \frac{C_{res}}{(1+i)^n} \quad (9)$$

where C_{ini} is the initial cost of each component, \$. d is the annual price degression rate of the corresponding component. j is the replacement number of the specific component and J is the total replacement number. l is the lifetime of the component. f_{mai} is the fixed proportion of the maintenance cost to the initial cost. C_{res} is the residual cost of the component.

$$PRV_{benefits} = PRV_{fit} + PRV_{tra} + PRV_{exp} + PRV_{car} \quad (10)$$

where PRV_{fit} is the FiT present value of the renewable system based on local regulations, \$.

PRV_{tra} is the present value of transmission loss saving, \$. PRV_{exp} is the present value of network expansion saving, \$. PRV_{car} is the present value of carbon reduction benefit, \$.

i. Feed-in tariff

The FiT subsidy of renewable energy has been implemented since 2018 in Hong Kong to encourage local renewable applications according to their installation capacity. For example, 3 HK\$/kWh will be paid annually to investors with the installed capacity larger than 200 kW but less than 1 MW until 2033 and generated electricity after that will be owned by investors [45]. The PV installations will therefore get two periods of the FiT subsidy (PRV_{fit_PV}) during the 20-year of service time including the first 13 years at the subsidy of the governmental FiT and the following 7 years at the subsidy of the local electricity tariff as shown in Eq. (11).

$$PRV_{fit\_PV} = \sum_{n=1}^{n=13} \frac{E_{PV} \cdot (1-\delta_{PV})^{n-1} \cdot c_{fit}}{(1+i)^n} + \sum_{n=14}^{n=20} \frac{E_{PV} \cdot (1-\delta_{PV})^{n-1} \cdot c_{ele} \cdot (1+\gamma)^{n-1}}{(1+i)^n} \quad (11)$$

where c_{fit} is FiT of renewable energy, \$/kWh. c_{ele} is the average electricity tariff of residential buildings, \$/kWh. γ is the annual escalation rate of local electricity price.

The FiT of the wind energy (PRV_{fit_WT}) is calculated with the rate of local electricity price (c_{ele}) as shown in Eq. (12).

$$PRV_{fit\_WT} = \sum_{n=1}^{n=20} \frac{E_{WT} \cdot (1-\delta_{WT})^{n-1} \cdot c_{ele} \cdot (1+\gamma)^{n-1}}{(1+i)^n} \quad (12)$$

ii. Transmission loss saving

The current fuel mix in Hong Kong mainly consists of coal, natural and nuclear energy, which generate electricity in remote plants far away from populated regions. So electricity supplied to high-rise residential buildings needs to be transmitted and distributed via underground cables and overhead lines. It is reported that the average transmission loss in Hong Kong during 2010 to 2014 is about 13.541% of the electricity output [35], and this part of the energy loss can be saved using the BIPV system as shown in Eq. (13).

$$PRV_{tra} = \sum_{n=1}^{n=20} \frac{f_{tra} \cdot c_{ele} \cdot E_{PV} \cdot (1-\delta_{PV})^{n-1} \cdot (1+\gamma)^{n-1}}{(1+i)^n} \quad (13)$$

where f_{tra} is the proportion of the transmission loss to the generated electricity.

iii. Network expansion saving

In order to meet the increasing demand of electricity consumption in different sectors, extra investment is needed to expand the utility network and infrastructure. It is reported by China Light and Power Hong Kong Limited that: 24% of the capital investment is spent on meeting the electricity demand of new developments and corresponding infrastructures; 38% of the capital investment is on maintaining the supply reliability; another 30% is on carbon emission reduction projects; and the remaining 8% is on smart city and digital technologies [46]. The development of renewable energy systems for building applications can save such network expansion costs as shown in Eq. (14).

$$PRV_{exp} = \sum_{n=1}^{n=20} \frac{f_{exp} \cdot c_{ele} \cdot (E_{PV} \cdot (1-\delta_{PV})^{n-1} + E_{WT} \cdot (1-\delta_{WT})^{n-1}) \cdot (1+\gamma)^{n-1}}{(1+i)^n} \quad (14)$$

where f_{exp} is ratio of cost on the network expansion to the total electricity investment.

iv. Carbon reduction benefit

A climate action plan has been launched in Hong Kong to keep pace with the Paris Agreement to control the carbon emission. It is projected to decrease the carbon footprint to about 3.3 - 3.8 tonnes/capita by 2030, leading to a reduction by 65% - 70% compared with that in 2005 [2]. The electricity consumption by the building sector in Hong Kong contributes to over 60% of carbon emissions, which can be significantly reduced by using renewable energy as calculated by Eq. (15).

$$PRV_{car} = \sum_{n=1}^{n=20} \frac{f_{car} \cdot c_{car} \cdot (E_{PV} \cdot (1-\delta_{PV})^{n-1} + E_{WT} \cdot (1-\delta_{WT})^{n-1})}{(1+i)^n} \quad (15)$$

where f_{car} is the local carbon intensity of electricity, $kgCO_2/kWh$. c_{car} is the societal cost of carbon, $\$/kgCO_2$.

3. Results and discussion

This section firstly analyzes test results of the PV-battery system to demonstrate the real system operational performance and validate the energy balance based battery model and energy management strategy for TRNSYS modelling. And the technical and economic performances of four typical application scenarios of renewable energy systems for power supply to the high-rise residential building in Hong Kong are then subject to detailed comparisons and discussions.

3.1. Experimental results and model validation of the PV-battery system

Three days' dynamic experimental data including the PV power, load power and grid power under both the maximizing self-consumption strategy and time-of-use strategy are collected and then used as the input parameters to the corresponding TRNSYS model. The power flow data for the maximizing self-consumption strategy on 15 December and time-of-use strategy on 18 December are selected for demonstration given its comprehensiveness compared with the other two testing days. The battery is controlled to be firstly charged and then discharged under the maximizing self-consumption strategy as shown in Fig. 7. And the PV-battery system experiences peak-flat-valley pricing periods under the time-of-use strategy as shown in Fig. 8. The convergence of the battery SOC between the test and modelling results is analyzed and discussed.

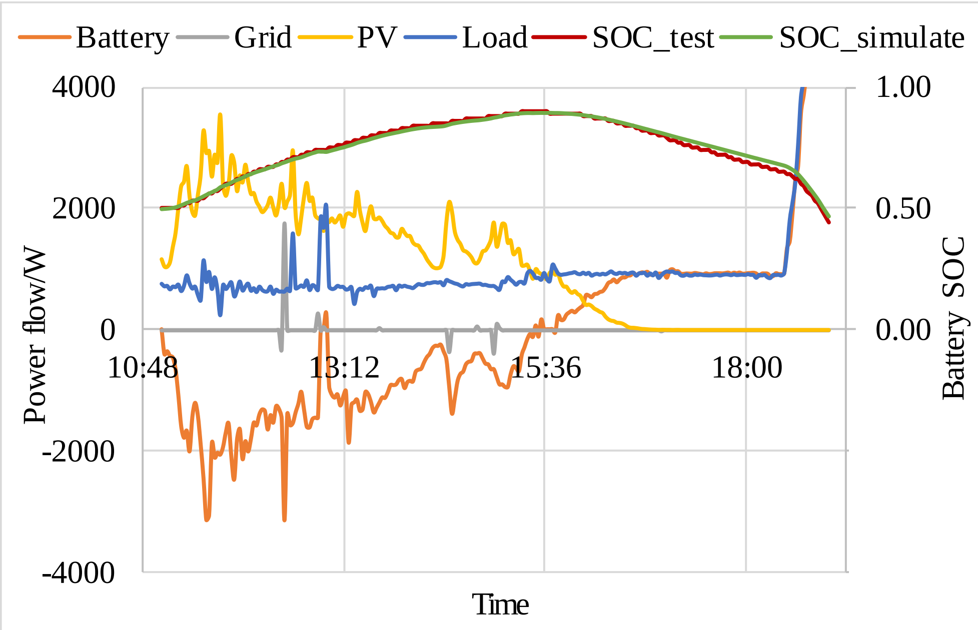

Fig. 7 Power flow and battery SOC of maximizing self-consumption strategy

Fig. 7 shows the distribution of the power flow and battery SOC for the PV-battery system under the maximizing self-consumption strategy. The PV self-consumption and load cover ratios are 98.5% and 99.3% in the maximizing self-consumption strategy, while these ratios decrease to 69.8% and 62.5% without battery storage under the same power inputs and strategy. It indicates that battery storage is important to increase the PV power consumption and load cover ratio. The grid feed-in energy would increase from 0.365 kWh to 4.768 kWh if the battery storage is not used in the system, and energy supply from the grid would also rise from 0.58 kWh to 4.683 kWh without battery storage. The root mean square deviation and mean bias error between the tested and simulated battery SOC under the maximizing self-consumption strategy are 1.49% and 0.99% respectively with the maximum error deviation of about 0.03.

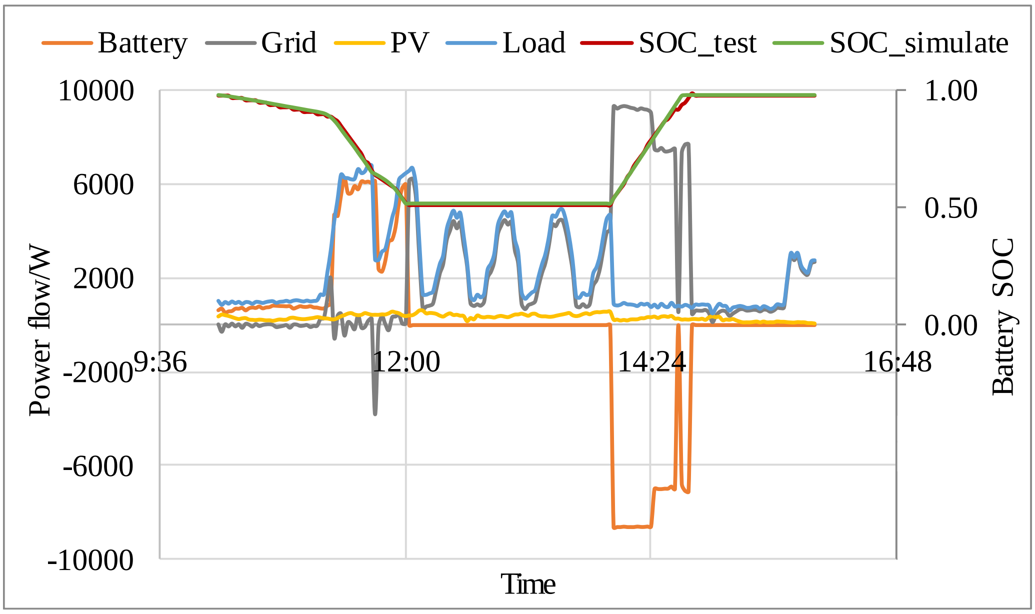

Fig. 8 Power flow and battery SOC of time-of-use strategy

The distribution of the power flow and battery SOC of the time-of-use strategy is shown in Fig. 8. The PV self-consumption ratio is 100% even there is no battery storage as the generated PV power is limited. But the load cover ratio increases from 19.7% to 44.0% with battery storage charged by the grid in the low-price period under the time-of-use strategy. The root mean square deviation and mean bias error between the tested and simulated SOC under the time-of-use strategy are 0.94% and 0.84% respectively. The maximum error deviation between the tested and simulated SOC is 0.04 when the battery SOC approaches its upper limit because the actual battery SOC is not theoretically accurate when almost fully charged.

3.2. Techno-economic feasibility of renewable energy applications for the typical high-rise building

The techno-economic feasibility of four typical application scenarios of renewable energy systems in the typical high-rise residential building is compared and discussed in this section.

3.2.1. Application scenario analyses and design optimization

Among different renewable application scenarios, the PV system is firstly developed for the high-rise residential building with both rooftop and façade PV panel installations (Case 1). In order to achieve an annual energy balance between the building demand and renewable power supply, the PV is coupled with wind power to generate more renewable power (Case 2). The battery storage is further added to the energy-balanced scenario to improve the load matching (Case 3). A holistic optimization case to size the wind and battery capacity for a techno-economic optimum solution is finally conduced in Case 4. The detailed economic parameters for the cost feasibility assessment are shown in Table 6.

Table 6 Parameters for economic assessment

Parameter	Value
Real discount rate (i)	5.8%/year [16]
Price degression rate (d)	4.5%/year [16]
PV degradation (δ_{PV})	1%/year [47]
Wind turbine degradation (δ_{WT})	1.5%/year [48]
Electricity tariff (c_{ele})	0.145 $/kWh [49]
Electricity price rising rate (γ)	1.4%/year [46]
Feed-in tariff (c_{fit})	0.3846 $/kWh [45]
Transmission loss ratio (f_{tra})	13.54% [35]
Network expansion ratio (f_{exp})	24% [46]
Carbon intensity of electricity (f_{car})	0.66 kgCO_2/kWh [50]
Societal cost of carbon (c_{car})	0.024 $/kg$CO_2$ [51]

The number of wind turbines in Case 2 and Case 3 based on the annual demand-supply balance is calculated to be 6. The optimum battery capacity in Case 3 is then obtained from a trade-off between the integrated technical and economic criteria. And an optimum solution of 1,080 kWh is derived from the minimum distance to the utopia point method [52]. To optimally size the wind and battery capacity of the hybrid PV-wind-battery system in Case 4, the multi-objective optimization work with the integrated technical criterion and economic criterion (LCOE) are developed to achieve the Pareto frontier (Fig. 9). It indicates an obvious trade-off conflict where the integrated technical criterion increases as the economic criterion decreases. The optimum solution as highlighted with the blue triangle is obtained by the minimum distance to the utopia point method with a battery capacity of 1,680 kWh and 10 wind turbines. It can achieve the optimum performance in both integrated technical criterion (considering the energy supply, battery storage, building demand and grid integration) and the economic criterion (LCOE with detailed benefits). Sensitivity analyses on the battery and wind turbine capacities are further conducted to examine their impact on each system performance indicator.

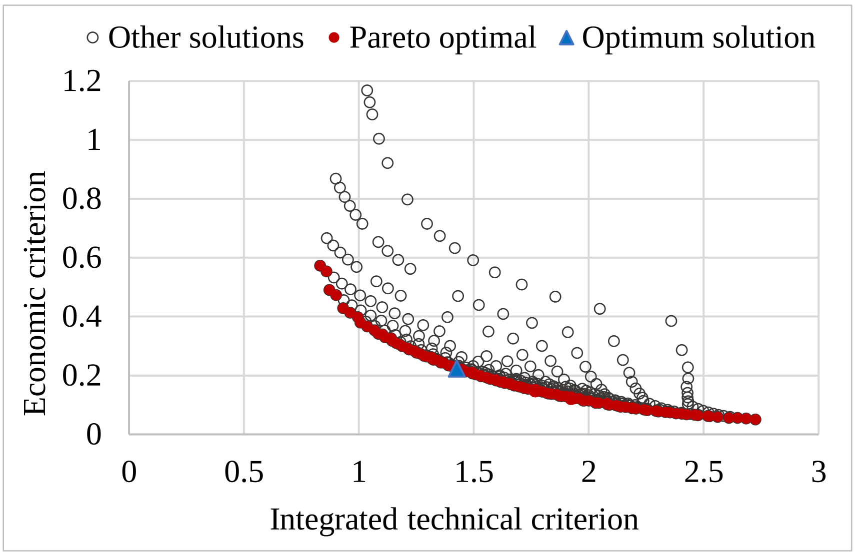

Fig. 9 Distribution of Pareto frontier of technical and economic criteria in Case 4

The impact of the battery capacity on the economic indicator (LCOE) and technical indicators including the load cover ratio (LCR), renewable energy self-consumption ratio (SCR), battery cycling aging (Aging), and standard deviation of net grid power (STD) is illustrated in Fig. 10. The wind turbine number is kept at the optimum value obtained in Case 4 (i.e. 10). Both SCR and LCR show increasing trends with the increased battery capacity as the magnitude of energy from renewable sources to the battery and energy from the battery to the load increases while the renewable energy generation and building load do not change with the battery capacity. Battery cycling aging decreases with growing battery capacity and the net grid power exchange is more stabilized with the rising batteries. The LCOE also increases with the rising battery capacity for higher investment.

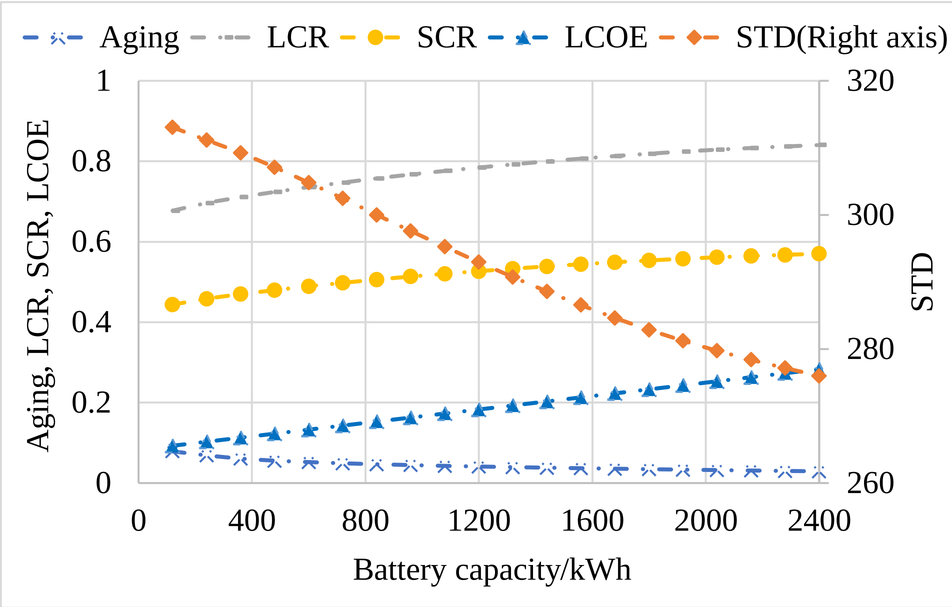

Fig. 10 Impact of battery capacity on the optimization indicators

The impact of the wind turbine number on the five optimization indicators with a fixed battery capacity of 1,680 kWh (the optimum solution in Case 4) is shown in Fig. 11. Both LCR and STD are positively related to the wind turbine number with larger renewable energy generation. The SCR decreases with the rising number of wind turbines with more available renewable energy generation, and the LCOE also decreases with the increasing wind turbines as wind power requires lower investment than PV [31, 53]. The battery cycling aging is firstly positively and then negatively related to the wind turbine number because both charging and discharging affect the battery cycling aging performance.

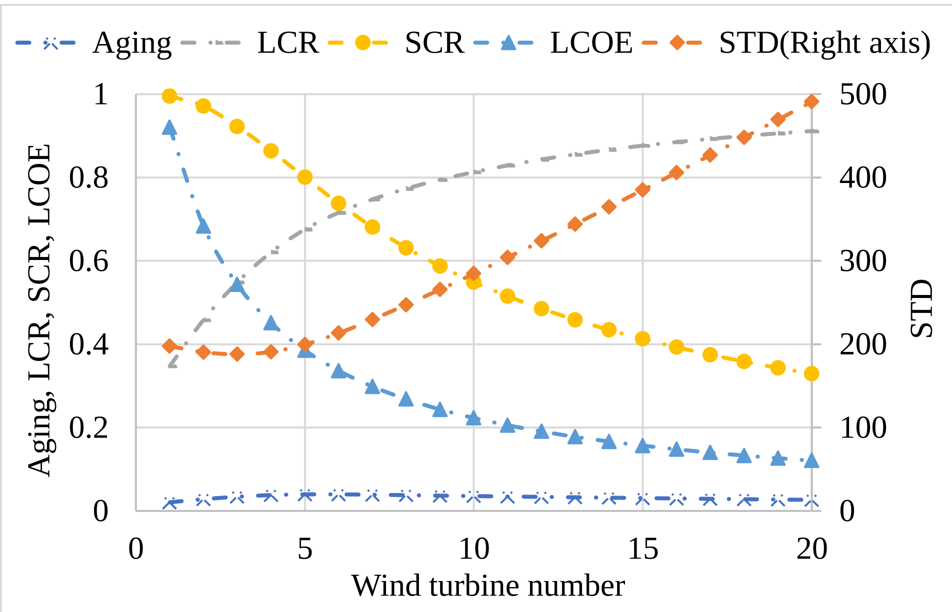

Fig. 11 Impact of wind turbine number on the optimization indicators

The sizing and optimization results of all four application scenarios are summarized in Table 7. The PV capacity of these cases keeps at 876.71 kW which is determined by the building layout with a maximum availability assumption. Detailed technical and economic performances of these four scenarios are explained in Section 3.2.2 and Section 3.2.3.

Table 7 System sizing results of four renewable application scenarios

System sizing	Case 1	Case 2	Case 3	Case 4
Wind turbine /number	0	6 (energy balance)	6 (energy balance)	10 (optimized)
Battery/kWh	0	0	1,080 (optimized)	1,680 (optimized)

3.2.2. Technical analysis of renewable energy applications

The technical performance of four application scenarios in the high-rise residential building is analyzed in this section. The power flow distributions of the renewable energy systems in a typical week (the third week in June) and each month are present for each case while the annual load cover and renewable energy self-consumption performance are compared among four cases.

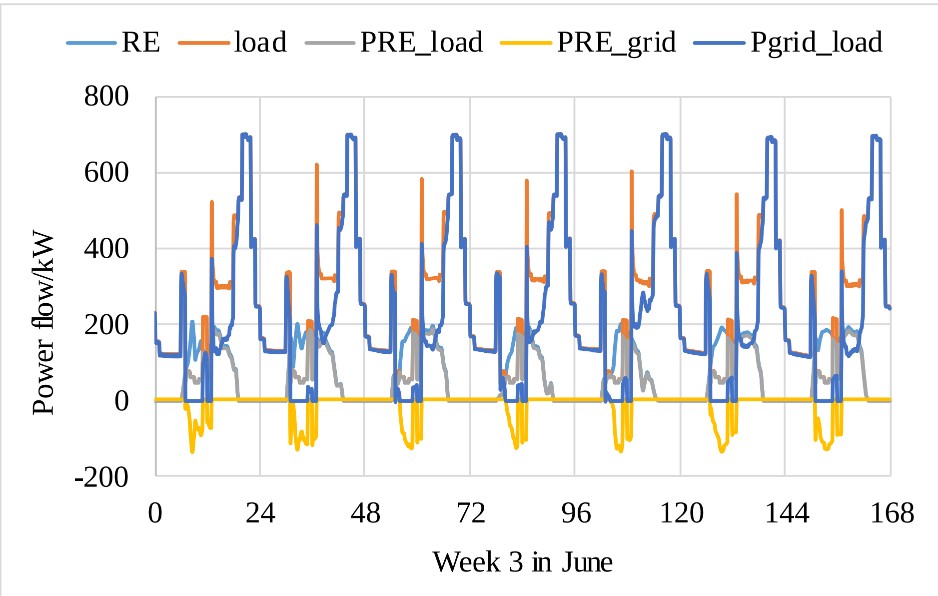

Fig. 12 Power flow of the PV system in the typical week in Case 1

The power flow of the PV system (Case 1) for building applications in the third week of June is presented in Fig. 12. The total weekly electrical load of the high-rise building is about 44,514.35 kWh while the PV generation in this week is 11,171.15 kWh with its 74.92% fed into the building load. The remaining 25.08% of renewable energy is fed into the grid even though the building load cannot be fully covered. The observed mismatch between the renewable generation and building electrical load echoes with findings in an existing research study [54]. The PV supply can only cover 18.80% of the weekly load in the typical high-rise building, so that the grid undertakes the left burden with a maximum grid transmission power of 699.97 kW (grid export as positive power and grid import as negative power).

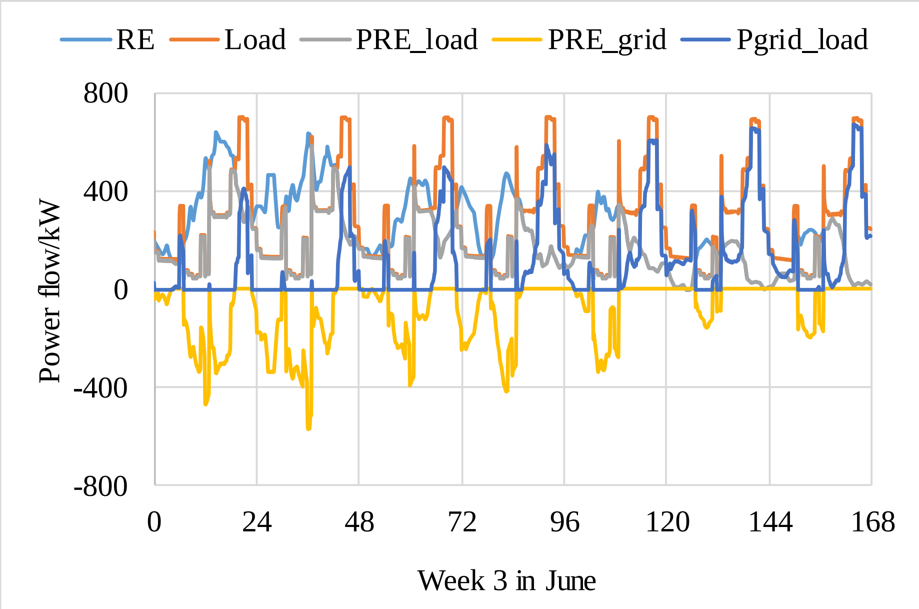

Fig. 13 Power flow of the PV-wind system in the typical week in Case 2

When the PV is combined with wind power to keep an energy balance between the annual demand and supply (Case 2), more renewable energy will be available with a weekly renewable energy generation of 40,585.03 kWh covering 57.41% of the weekly load as shown in Fig. 13. The average renewable energy self-consumption ratio in this week is about 62.97% and more renewable energy will be fed into the utility grid. The grid will cover much less weekly electrical load (for 42.59%) compared with Case 1, with a maximum grid transmission power of 676.82 kW.

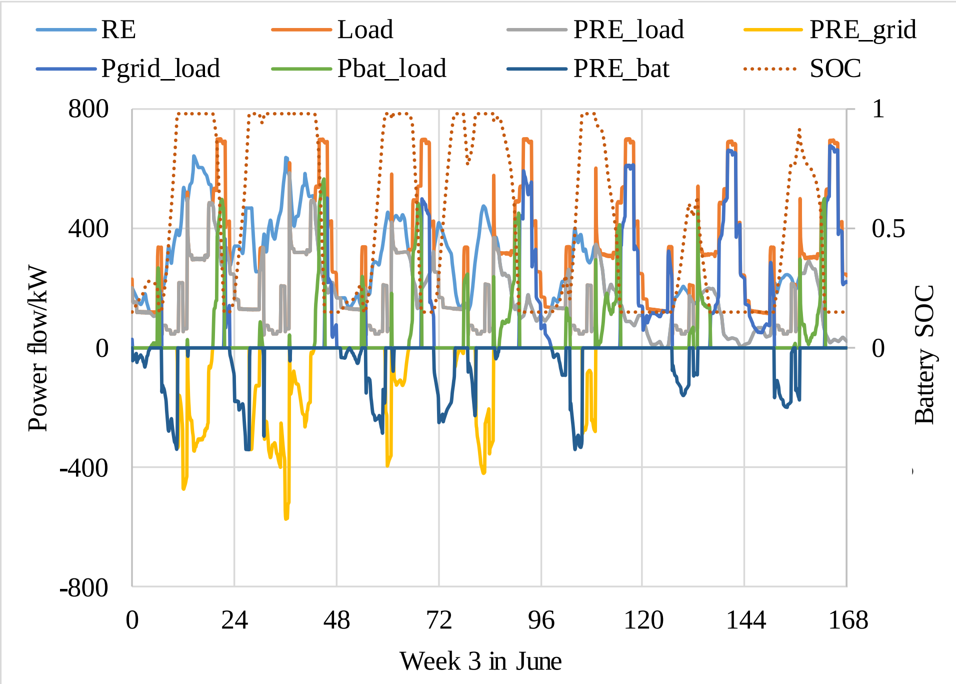

Fig. 14 Power flow of the PV-wind-battery system in the typical week in Case 3

When battery storage is included in Case 3 for the energy-balanced scenario with an optimum techno-economic performance, the PV-wind-battery system can cover 69.68% of the electrical load in this typical week which is higher than that in Case 1 and Case 2 as shown in Fig. 14. The battery storage undertakes 12.27% of the weekly load which needs to be covered by the grid in Case 2 (battery discharging as positive power and battery charging as negative power). The utility grid will cover the remaining 30.32% weekly load with the maximum grid transmission power of 676.82 kW. The maximum grid transmission power in Case 2 and Case 3 is the same as the renewable energy generation in these two cases is the same and the grid is controlled to cover the unsatisfied load when battery discharging is not available. The weekly self-consumption ratio of the system is about 79.12% which is higher than that in Case 2 with 16.15% renewable power charging the battery. It is validated that the battery storage can increase the load matching and self-consumption performance of the system to a large extent as reported in Ref. [55].

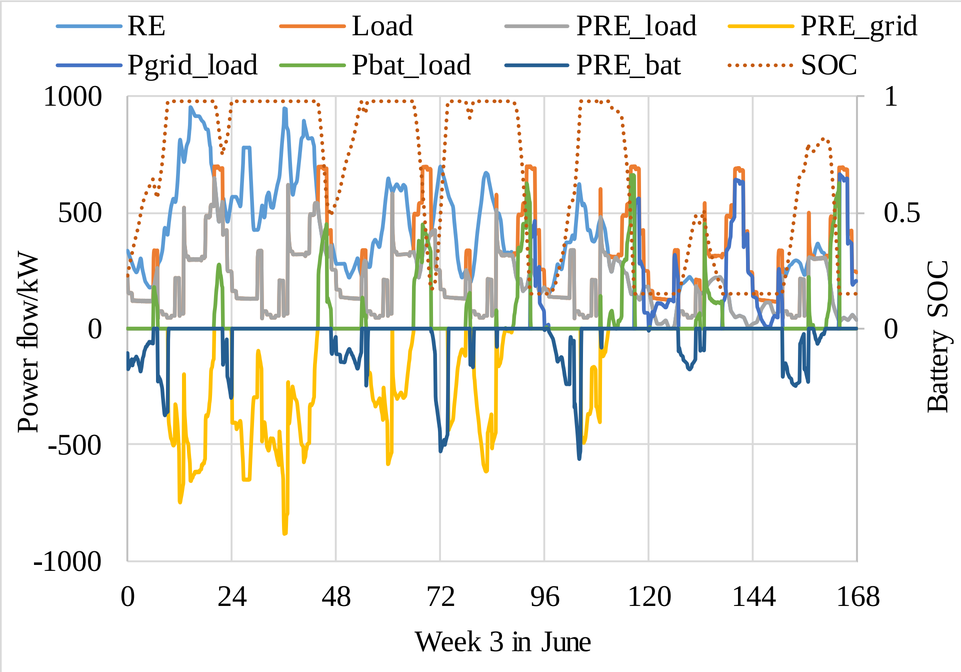

Fig. 15 Power flow of the PV-wind-battery system in the typical week in Case 4

The wind power and battery storage are simultaneously optimized in Case 4 to find a comprehensive techno-economic optimum solution for the high-rise building as shown in Fig. 15. It indicates that the hybrid PV-wind-battery system covers the majority (i.e. 82.57%) of the total load in the typical week with 14.14% from battery storage. And the grid only needs to cover 17.43% of the weekly load with the maximum grid transmission power of -885.15 kW (grid import) as a large amount of renewable energy is available in the optimum hybrid system.

The monthly energy flow and load matching performance of four application cases is illustrated in Fig. 16. It is indicated that the building electrical load in summer is relatively higher than that in winter due to a large cooling load in the hot summer and warm winter region. In Case 1 with the BIPV, both monthly PV generation and building load achieve the maximum value in July for 47.15 MWh and 196.84 MWh and the maximum monthly LCR is 18.47% on November. The monthly LCR significantly increases in Case 2 with the application of wind power and the maximum LCR is about 60.04% in March. With the application of battery storage in Case 3, the monthly LCR can be further increased on top of Case 2 reaching a maximum of 79.03% in March. The monthly LCR shows a rising trend in Case 4 with increased wind turbines and batteries compared with Case 3 and the maximum LCR reaches up to 90.32% in March. An obvious seasonal difference on LCR can be observed when wind turbines are introduced in Case 2, 3 and 4 with a minimum value in July and maximum value in March as dependent on the wind power generation.

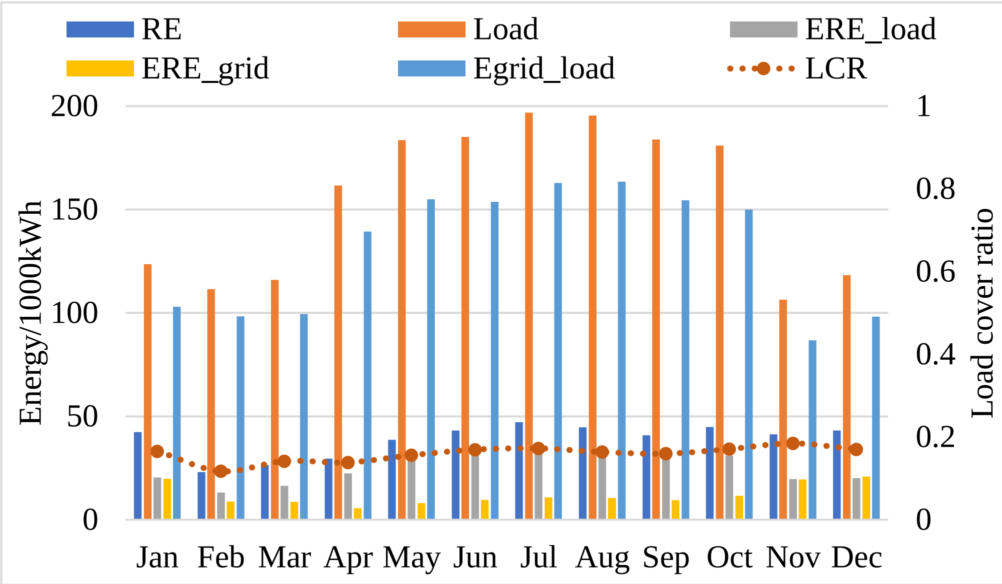

Fig. 16(a) Monthly energy flow and load matching in Case 1

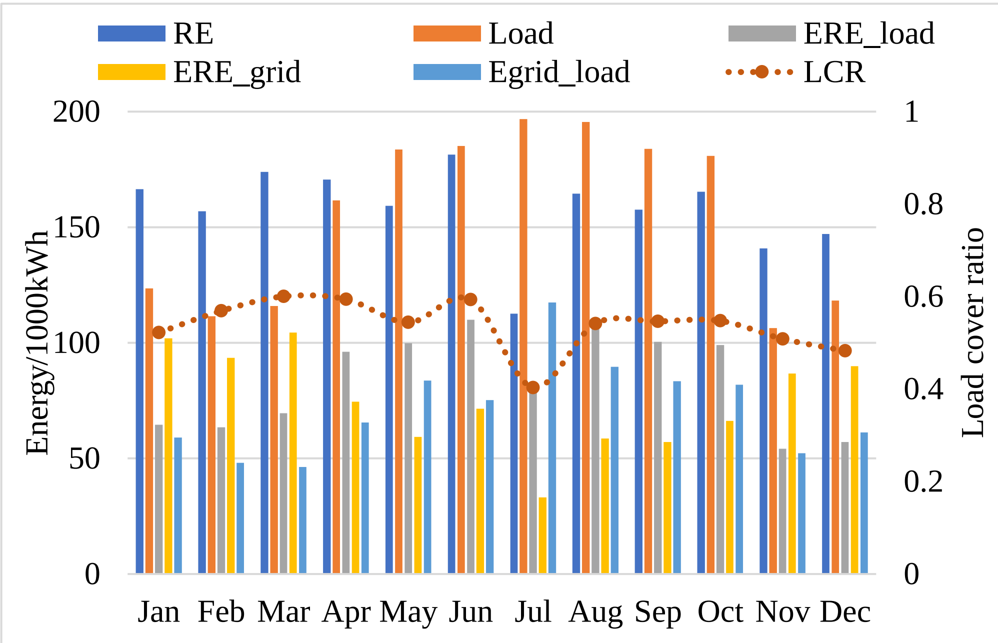

Fig. 16(b) Monthly energy flow and load matching in Case 2

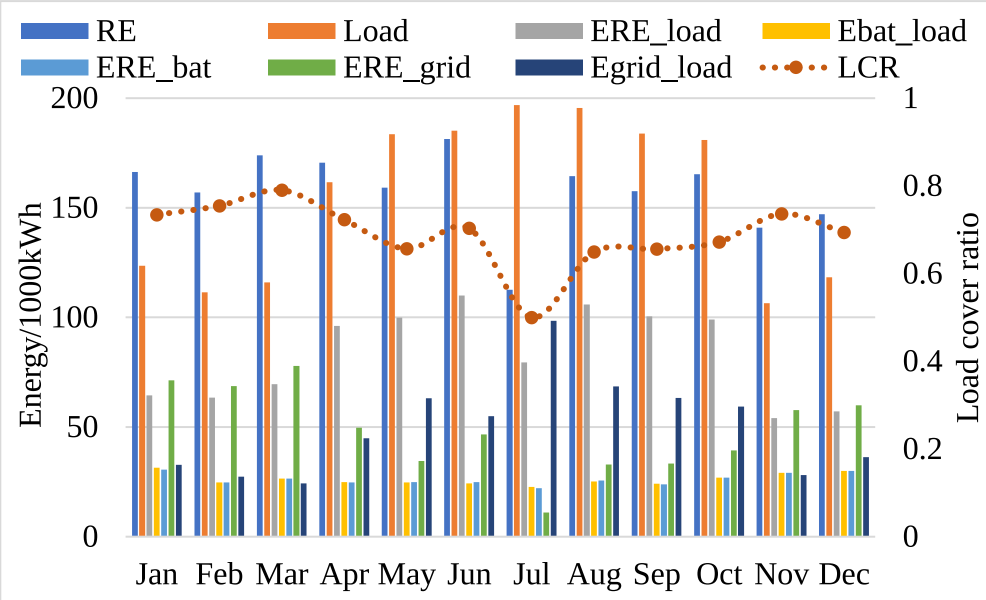

Fig. 16(c) Monthly energy flow and load matching in Case 3

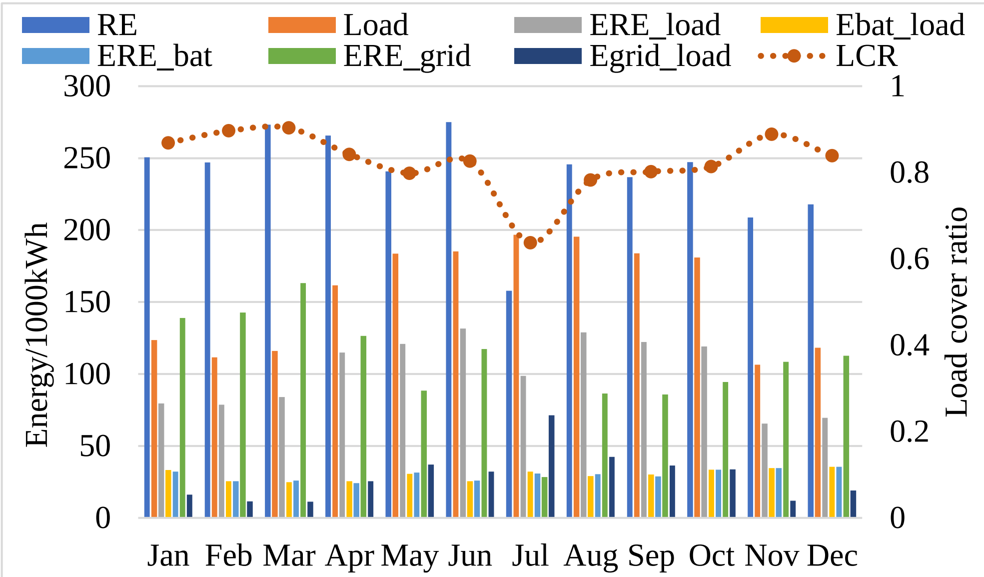

Fig. 16(d) Monthly energy flow and load matching in Case 4

The annual average load cover ratio of these four cases is compared in Fig. 17. The annual average load cover ratio can be increased from 16.02% in Case 1 to 53.65% in Case 2 when wind power is introduced to the system. The mismatch between the renewable power generation and the building load is obvious as shown in Case 2, where 46.35% of the annual load is taken by the grid. The battery storage can therefore help cover another 14.08% of the annual load in Case 3, further reducing the reliance on the grid. Finally, the comprehensive optimum scenario as studied in Case 4 covers the majority of the annual load of 81.29%.

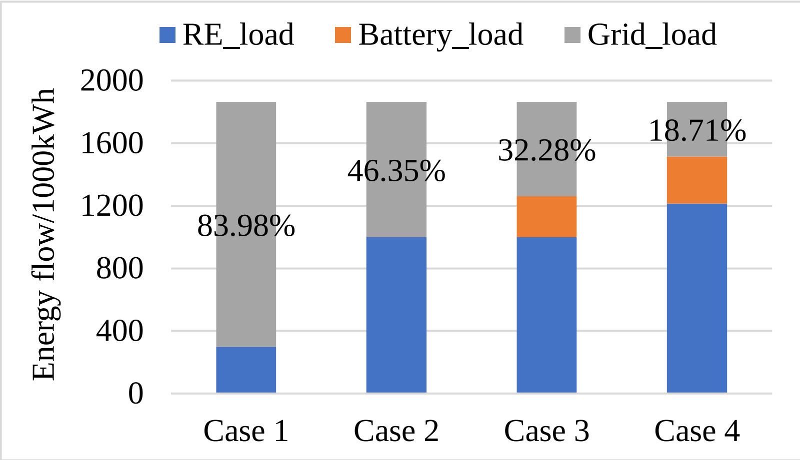

Fig. 17 Annual average load cover ratio of four cases

Fig. 18 compares the annual average renewable energy self-consumption ratio across four studied cases. It is indicated that 67.59% of the PV generation is directed to meet the building load with the other 32.41% fed into the grid in Case 1. With the increase of renewable energy generation, the import energy into the grid increases as shown in Case 2 and Case 4. And batteries store about 16.56% of renewable generation in Case 3 which is originally fed into the grid in Case 2. The self-consumption ratio of the optimum PV-wind-battery system in Case 4 is 54.89% with the other 45.11% of renewable energy fed into the grid.

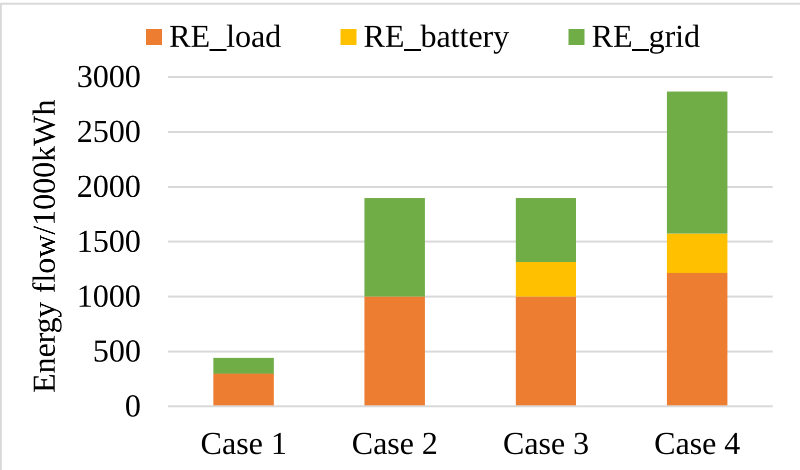

Fig. 18 Annual average renewable energy self-consumption ratio of four cases

Battery aging after one-year operation in Case 3 is about 4.85% and the battery state of health is about 99.03% of rated capacity. Battery aging in Case 4 is further reduced to 3.568% since a larger battery capacity is employed and the battery state of health is improved to about 99.28% of the rated capacity. As for the grid integration performance, the standard deviation of net grid power increases with more renewable energy generation, while the battery storage contributes to reducing the standard deviation as compared between Case 2 and Case 3.

3.2.3. Economic analysis of renewable energy applications

The economic performance of four renewable energy systems is further analyzed in this section. The lifetime present value considering the investment costs and detailed benefits is compared in Fig. 19. The investment of the renewable energy systems increases from Case 1 to Case 4 as wind turbines are installed in Case 2 and batteries are matched for Case 3, while the optimized wind turbine and battery capacity are the maximum in Case 4. The initial cost ratios of the major investment for four cases are 77.34%, 80.18%, 69.18% and 68.09% respectively. The benefits of the renewable application in Case 2 and Case 3 are the same as per renewable energy generation. The FiT subsidy of the renewable application dominates the total gained benefits with 81.42%, 76.59%, 76.59% and 75.70% respectively in the four cases.

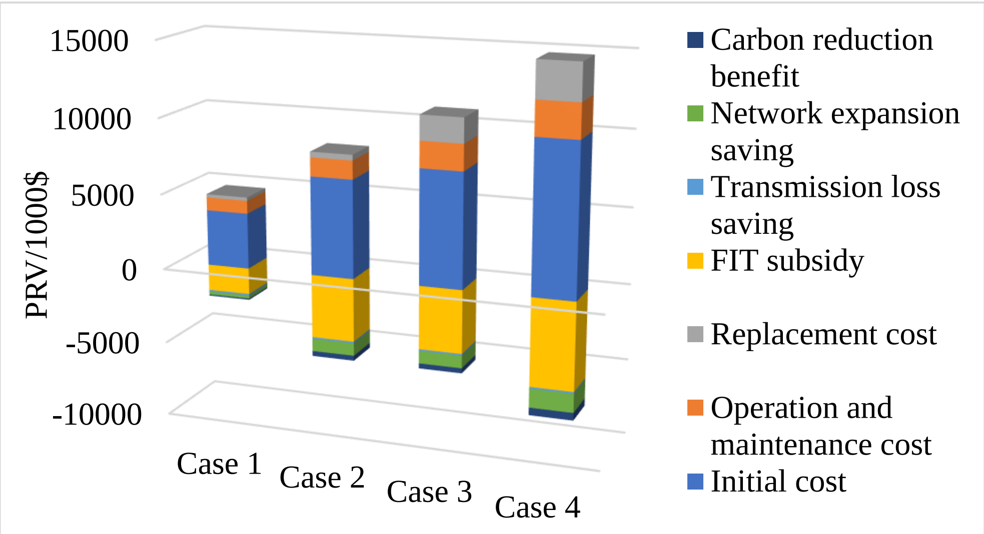

Fig. 19 Lifetime present value of four typical renewable application scenarios

The detailed PRV and LCOE of the four typical renewable application scenarios are summarized in Table 8. It shows that the LCOE of the PV system in Case 1 is 0.5252 $/kWh which is higher than the reported result of PV applications in Hong Kong for 0.2609 $/kWh [31] as the energy generation of the façade PV is impaired by adjacent shading. The LCOE of the PV-wind system in Case 2 is 0.1251 $/kWh as wind power requires lower investment than PV applied in Hong Kong [31, 53]. The LCOE in Case 3 increases to 0.2610 $/kWh with the application of batteries at a relatively higher cost. And the LCOE of the optimum PV-wind-battery system in Case 4 is about 0.2230 $/kWh which is lower than the reported result of 0.42 $/kWh conducted in Korea [38], as a large amount of FiT subsidies available in Hong Kong and other renewable energy benefits including the transmission loss saving, network expansion saving and carbon reduction benefit are considered in this study. Furthermore, the LCOE of PV-wind-battery systems is expected to be further reduced as the lithium battery cost is showing a steady decreasing trend in recent years [9].

Table 8 PRV and LCOE of four typical renewable energy scenarios

PRV and LCOE	Case 1	Case 2	Case 3	Case 4
Initial cost $	3,682,182	6,502,182	7,582,182	10,062,182
Operation and maintenance cost $	858,574	1,236,309	1,739,956	2,271,584
Replacement cost $	220,359	371,168	1,638,497	2,443,109
FIT subsidy $	-1,727,839	-4,200,066	-4,200,066	-5,848,217
Transmission line saving $	-113,484	-113,484	-113,484	-113,484
Network expansion saving $	-201,139	-838,104	-838,104	-1,262,747
Carbon reduction benefit $	-79,592	-332,370	-332,370	-500,888
System LCOE $/kWh	0.5252	0.1251	0.2610	0.2230

4. Conclusions

This study analyzes the techno-economic feasibility of four typical scenarios of renewable energy applications for power supply to a high-rise residential building in Hong Kong. Experiments on the PV-battery system under the maximizing self-consumption and time-of-use strategies are conducted to investigate the system operational performance and validate the energy balance based battery model and energy management strategy in TRNSYS modelling. The integrated technical optimization criterion focusing on the performance of four major system components (energy supply, battery storage, building demand and grid relief) and the improved LCOE considering detailed renewables benefits (FiT subsidy, transmission loss saving, network expansion saving and carbon reduction benefit) are developed for design optimizations of renewable energy systems. Important findings are concluded as below:

(1) The root mean square deviations between the tested and simulated battery SOC for the maximizing self-consumption and time-of-use strategies are 1.49% and 0.94% respectively. And the maximum error deviations between the tested and simulated SOC for these two strategies are 0.03 and 0.04, which successfully validated the energy balance based battery model and energy management strategy in TRNSYS modelling.

(2) The technical feasibility of four typical renewable application scenarios for high-rise residential buildings is clarified. The PV system in Case 1 can cover 16.02% of the annual building electrical load while the PV-wind system with balanced annual supply and demand in Case 2 covers 53.65% of the annual load. The PV-wind-battery system with balanced annual supply and demand in Case 3 can further satisfy 69.26% of the annual load and relieve the utility grid stress. The battery storage can improve the annual average load cover and self-consumption ratios by 14.08% and 16.56% as compared in Case 2 and Case 3. The optimum PV-wind-battery system in Case 4 can cover the majority of total annual load of 81.29% with a simultaneous consideration of the battery health protection and grid relief.

(3) The LCOE of the PV system in Case 1 is about 0.5252 $/kWh as the adjacent shading impairs the energy generation of façade PV. The LCOE of the PV-wind system (0.1251 $/kWh) with a balanced annual supply and demand in Case 2 is the lowest in four scenarios, while it increases to 0.2610 $/kWh after battery storage is coupled with the renewable system in Case 3. The LCOE of the optimum hybrid PV-wind-battery system in Case 4 is predicted to be 0.2230 $/kWh, which can be further reduced with the declining price of the lithium-ion battery.

(4) It is suggested that the application of PV-wind systems in high-rise residential buildings in Hong Kong is feasible with a low LCOE while the PV-wind-battery systems can contribute to higher building energy autonomy with an affordable cost. The techno-economic feasibility of these typical renewable application scenarios can provide relative stakeholders critical references to facilitate the renewable penetration into high-density urban areas and therefore help change the current fuel mix for power generation in Hong Kong and other similar regions.

Nomenclature

Acronyms

aNSGA-II type: Active Archive Non-dominated Sorting Genetic Algorithm

BIPV: building-integrated photovoltaic

CSA: crow search algorithm

EMS: energy management strategy

FC: fuel cell

FiT: feed-in tariff

GA-PSO: genetic algorithm with particle swarm optimization

LCR: load cover ratio

LCOE: levelized cost of energy

LPSP: loss of power supply probability

MOEA/D: evolutionary algorithm based on decomposition

MOPSO: multi-objective particle swarm optimization

PRV: present value

NSGA-II: Non-dominated Sorting Genetic Algorithm-II

PV: photovoltaic

RE: renewable energy

SCR: self-consumption ratio

SOC: state of charge

SOH: state of health

STD: standard deviation

WT: wind turbine

List of symbols

$Battery_{rated}$: battery rated capacity, kWh

c_{car}: societal cost of carbon, $/kgCO_2$

c_{ele}: electricity tariff of residential buildings, $/kWh

c_{fit}: feed-in tariff of renewable energy, $/kWh

C_{ini}: initial cost of the component, $

C_{res}: residual cost of the component, $

d: annual price degression rate of the component

$E_{battery\ to\ load}$: battery electricity discharged to the building load, kWh

E_{load}: annul electrical load of the building, kWh

E_{PV}: PV energy generation in the first year, kWh

$Equ_{lifecycle}$: battery equivalent lifecycle number

E_{RE_load}: annual electricity from the renewable generation to the building load, kWh

$E_{RE\_battery}$: annual renewable electricity to charge the battery, kWh

E_{RE}: annual renewable generation, kWh

E_{WT}: wind energy generation in the first year, kWh

f_{car}: local carbon intensity of electricity, $kgCO_2/kWh$

f_{exp}: ratio of cost on the network expansion to the total electricity investment

f_{mai}: fixed proportion of the maintenance cost to the initial cost

f_{tra}: proportion of the transmission loss to the generated electricity

j: replace number of the component

J: total replace number of the component

i: annual real discount rate

l: lifetime of the component

n: a certain year in the lifetime

N: service lifetime of the renewable system

$P_{battery}$: battery power flow in the charge and discharge process, kW

$P_{grid\ to\ load}$: grid exported power to meet the electrical load, kW

$P_{RE\ to\ grid}$: renewable power fed into the utility grid, kW

$PRV_{benefits}$: present value of the potential benefits of renewable energy systems, $

PRV_{car}: present value of the carbon reduction benefit, $.

PRV_{costs}: present value of the investment costs, $

PRV_{exp}: present value of the network expansion saving, $

PRV_{fit}: feed-in tariff present value of the renewable system, $

PRV_{tra}: present value of the transmission loss saving, $

$Technical_{optimal}$: integrated technical optimization criterion

ΣE_{RE}: system renewable energy generation during the service time, kWh

δ_{PV}: annual degradation rate of the PV system

δ_{WT}: annual degradation rate of the wind turbine system

γ: annual escalation rate of local electricity price

Acknowledgement

The work described in this paper was financially supported by the National Key R&D Program of China, Research and integrated demonstration on suitable technology of net zero energy building (Project No.: 2019YFE0100300). This work is also supported by the RIF research project (RC2L) of the Research Grants Council, Hong Kong, China.

Reference

[1] United Nations. The Paris Agreement. 2015.

[2] Environment Bureau. Hong Kong's climate action plan 2030+. 2017.

[3] Moran D, Kanemoto K, Jiborn M, Wood R, Többen J, Seto KCJERL. Carbon footprints of 13 000 cities. 2018;13:064041.

[4] Elkadeem MR, Wang S, Sharshir SW, Atia EG. Feasibility analysis and techno-economic design of grid-isolated hybrid renewable energy system for electrification of agriculture and irrigation area: A case study in Dongola, Sudan. Energy Conversion and Management. 2019;196:1453-78.

[5] Li Y, Wang C, Li G, Wang J, Zhao D, Chen C. Improving operational flexibility of integrated energy system with uncertain renewable generations considering thermal inertia of buildings. Energy Conversion and Management. 2020;207:112526.

[6] Ma W, Xue X, Liu G, Zhou R. Techno-economic evaluation of a community-based hybrid renewable energy system considering site-specific nature. Energy Conversion and Management. 2018;171:1737-48.

[7] Zhou Y, Cao S. Energy flexibility investigation of advanced grid-responsive energy control strategies with the static battery and electric vehicles: A case study of a high-rise office building in Hong Kong. Energy Conversion and Management. 2019;199:111888.

[8] Llamas B, Ortega MF, Barthelemy G, de Godos I, Acién FG. Development of an efficient and sustainable energy storage system by hybridization of compressed air and biogas technologies (BIO-CAES). Energy Conversion and Management. 2020;210:112695.

[9] REN 21. Renewables 2019 global status report-renewable electricity generation costs. 2019.

[10] Sierra club. Los Angeles is now committed to 100% clean, renewable energy community-wide. 2019.

[11] Liu J, Chen X, Cao S, Yang H. Overview on hybrid solar photovoltaic-electrical energy storage technologies for power supply to buildings. Energy Conversion and Management. 2019;187:103-21.

[12] Ruusu R, Cao S, Manrique Delgado B, Hasan A. Direct quantification of multiple-source energy flexibility in a residential building using a new model predictive high-level controller. Energy Conversion and Management. 2019;180:1109-28.

[13] Tumminia G, Guarino F, Longo S, Aloisio D, Cellura S, Sergi F, et al. Grid interaction and environmental impact of a net zero energy building. Energy Conversion and Management. 2020;203:112228.

[14] Yan J, Lu L, Ma T, Zhou Y, Zhao CY. Thermal management of the waste energy of a stand-alone hybrid PV-wind-battery power system in Hong Kong. Energy Conversion and Management. 2020;203:112261.

[15] Mazzeo D, Oliveti G, Baglivo C, Congedo PM. Energy reliability-constrained method for the multi-objective

optimization of a photovoltaic-wind hybrid system with battery storage. Energy. 2018;156:688-708.

[16] Bingham RD, Agelin-Chaab M, Rosen MA. Whole building optimization of a residential home with PV and battery storage in The Bahamas. Renewable Energy. 2019;132:1088-103.

[17] Salata F, Ciancio V, Dell'Olmo J, Golasi I, Palusci O, Coppi M. Effects of local conditions on the multi-variable and multi-objective energy optimization of residential buildings using genetic algorithms. Applied Energy. 2020;260:114289.

[18] Ferrara M, Rolfo A, Prunotto F, Fabrizio E. EDeSSOpt – Energy Demand and Supply Simultaneous Optimization for cost-optimized design: Application to a multi-family building. Applied Energy. 2019;236:1231-48.

[19] Waibel C, Evins R, Carmeliet J. Co-simulation and optimization of building geometry and multi-energy systems: Interdependencies in energy supply, energy demand and solar potentials. Applied Energy. 2019;242:1661-82.

[20] González-Mahecha RE, Lucena AFP, Szklo A, Ferreira P, Vaz AIF. Optimization model for evaluating on-site renewable technologies with storage in zero/nearly zero energy buildings. Energy and Buildings. 2018;172:505-16.

[21] Elkadeem MR, Wang S, Azmy AM, Atiya EG, Ullah Z, Sharshir SW. A systematic decision-making approach for planning and assessment of hybrid renewable energy-based microgrid with techno-economic optimization: A case study on an urban community in Egypt. Sustainable Cities and Society. 2020;54:102013.

[22] Ghorbani N, Kasaeian A, Toopshekan A, Bahrami L, Maghami A. Optimizing a hybrid wind-PV-battery system using GA-PSO and MOPSO for reducing cost and increasing reliability. Energy. 2018;154:581-91.

[23] Ghaffari A, Askarzadeh A. Design optimization of a hybrid system subject to reliability level and renewable energy penetration. Energy. 2020;193:116754.

[24] Ma T, Javed MS. Integrated sizing of hybrid PV-wind-battery system for remote island considering the saturation of each renewable energy resource. Energy Conversion and Management. 2019;182:178-90.

[25] Huang Z, Xie Z, Zhang C, Chan SH, Milewski J, Xie Y, et al. Modeling and multi-objective optimization of a stand-alone PV-hydrogen-retired EV battery hybrid energy system. Energy Conversion and Management. 2019;181:80-92.

[26] Hong Kong Housing Authority. Standard block typical floor plans. 2016.

[27] Chen H, Lee WL, Yik FWH. Applying water cooled air conditioners in residential buildings in Hong Kong. Energy Conversion and Management. 2008;49:1416-23.

[28] Hong Kong Building Environmental Assessment Method Society. An envrionmental assessment for new buildings Version 4/04. 2004.

[29] Hong Kong Electrical and Mechanical Services Department. Guidelines on Performance-based Building Energy Code. 2007.

[30] Wan KSY, Yik FWH. Building design and energy end-use characteristics of high-rise residential buildings in Hong Kong. Applied Energy. 2004;78:19-36.

[31] Peng J, Lu L. Investigation on the development potential of rooftop PV system in Hong Kong and its environmental benefits. Renewable and Sustainable Energy Reviews. 2013;27:149-62.

[32] Duffie JA, Beckman WA, Worek W. Solar engineering of thermal processes: Wiley Online Library; 2013.

[33] Chen X, Yang H, Peng J. Energy optimization of high-rise commercial buildings integrated with photovoltaic facades in urban context. Energy. 2019;172:1-17.

[34] Wind turbine models. Hummer H21.0-100kW. 2017.

[35] International Energy Agency Statistics. Electric power transmission and distribution losses (% of output) Hong Kong SAR, China. 2018.

[36] Jiang Y, Kang L, Liu Y. A unified model to optimize configuration of battery energy storage systems with

multiple types of batteries. Energy. 2019;176:552-60.
[37] Pena-Bello A, Barbour E, Gonzalez MC, Patel MK, Parra D. Optimized PV-coupled battery systems for combining applications: Impact of battery technology and geography. Renewable and Sustainable Energy Reviews. 2019;112:978-90.
[38] Jung W, Jeong J, Kim J, Chang D. Optimization of hybrid off-grid system consisting of renewables and Li-ion batteries. Journal of Power Sources. 2020;451:227754.
[39] Hamdy M, Nguyen A-T, Hensen JLM. A performance comparison of multi-objective optimization algorithms for solving nearly-zero-energy-building design problems. Energy and Buildings. 2016;121:57-71.
[40] Magnier L, Haghighat F. Multiobjective optimization of building design using TRNSYS simulations, genetic algorithm, and Artificial Neural Network. Building and Environment. 2010;45:739-46.
[41] Voss K, Sartori I, Napolitano A, Geier S, Gonçalves H, Hall M, et al. Load matching and grid interaction of net zero energy buildings. EUROSUN 2010 International Conference on Solar Heating, Cooling and Buildings2010.
[42] Delgarm N, Sajadi B, Delgarm S, Kowsary F. A novel approach for the simulation-based optimization of the buildings energy consumption using NSGA-II: Case study in Iran. Energy and Buildings. 2016;127:552-60.
[43] Chen X, Yang H. Integrated energy performance optimization of a passively designed high-rise residential building in different climatic zones of China. Applied Energy. 2018;215:145-58.
[44] Ma W, Fan J, Fang S, Liu G. Techno-economic potential evaluation of small-scale grid-connected renewable power systems in China. Energy Conversion and Management. 2019;196:430-42.
[45] Electrical and Mechanical Services Department. Introduction to feed-in tariff of renewable energy in Hong Kong. 2018.
[46] China Light and Power Hong Kong Limited. Electricity price adjustment. 2018.
[47] Campbell M AP, Blunden J, Smeloff E, Wright S. The Drivers of the Levelized Cost of Electricity for Utility-Scale Photovoltaics. SunPower Corp. 2008.
[48] Li J, Zhang X, Zhou X, Lu L. Reliability assessment of wind turbine bearing based on the degradation-Hidden-Markov model. Renewable Energy. 2019;132:1076-87.
[49] Global petrol prices. Hong Kong electricity prices. 2019.
[50] China Light and Power Hong Kong Limited. 2018 Annual report. 2018.
[51] Ricke K, Drouet L, Caldeira K, Tavoni M. Country-level social cost of carbon. Nature Climate Change. 2018;8:895-900.
[52] Chen X, Yang H, Sun K. A holistic passive design approach to optimize indoor environmental quality of a typical residential building in Hong Kong. Energy. 2016;113:267-81.
[53] Gao X, Yang H, Lu L. Investigation into the optimal wind turbine layout patterns for a Hong Kong offshore wind farm. Energy. 2014;73:430-42.
[54] Cao S, Sirén K. Impact of simulation time-resolution on the matching of PV production and household electric demand. Applied Energy. 2014;128:192-208.
[55] Liu J, Chen X, Yang H, Li Y. Energy storage and management system design optimization for a photovoltaic integrated low-energy building. Energy. 2020;190:116424.